Pseudo-goldstones as Light Dark Matter & First Order Phase Transitions

Andrea Addazi,
College of Science and Technology of Sichuan University
Laboratori Nazionali di Frascati INFN

This talk is based on several recent works, some of them listed above

AA, R. Pasechnik, A. Marciano, A. Morais, R. Srivastava, J.Valle, arXiv:1909.09740

AA, R. Pasechnik, A. Marciano, arXiv:1811.09074

AA, A. Marciano, A. Morais, R. Pasechnik et al, arXiv:2304.02399

AA, Y. Cai, Q. Gan, A. Marciano, K. Zeng, arXiv:2009.10327

AA, Y. Cai, A. Marciano, L. Visinelli, arXiv:2306.17205

Y. Aldabergenov, AA, S. Ketov, arXiv:2006.16641

Aknowledgements

National Science Foundation of China (NSFC) through the grant No. 12350410358;

Talent Scientific Research Program of College of Physics, Sichuan University, Grant No. 1082204112427

The Fostering Program in Disciplines Possessing Novel Features for Natural Science of Sichuan University, Grant No.2020SCUNL209

1000 Talent Tianfu program of Sichuan province 2021

Main idea in a mini-nutshell

Cold or Warm Dark Matter, still behaving better than MOND in observations such as Bullet Cluster

WIMPs à là “thermal miracle” are highly disfavoured by deep underground labs, colliders and indirect detection/cosmic rays

No new physics data in direct detection experiments demands for minimality as a cautious attitude, minimalism and Occam’s razor

Searching for Alternative Candidates for Dark Matter beyond “standard WIMPs

Sorry for missing references but these are very well known facts and statements

Extra U(1) beyond SM symmetry

Gauge: B-L,D,…,X

Dark Photons, Baryo-photons, extra Z', etc.

Global: L, B-L, B,PQ,…,X

Pseudo-bosons bosons:
Majorons, Axions, …

Globals need for a spontaneous symmetry breaking and a new VEV

$$\sigma = Re\sigma + iIm\sigma$$

Pseudo-Goldstone as Dark Particle

First Order Phase Transitions

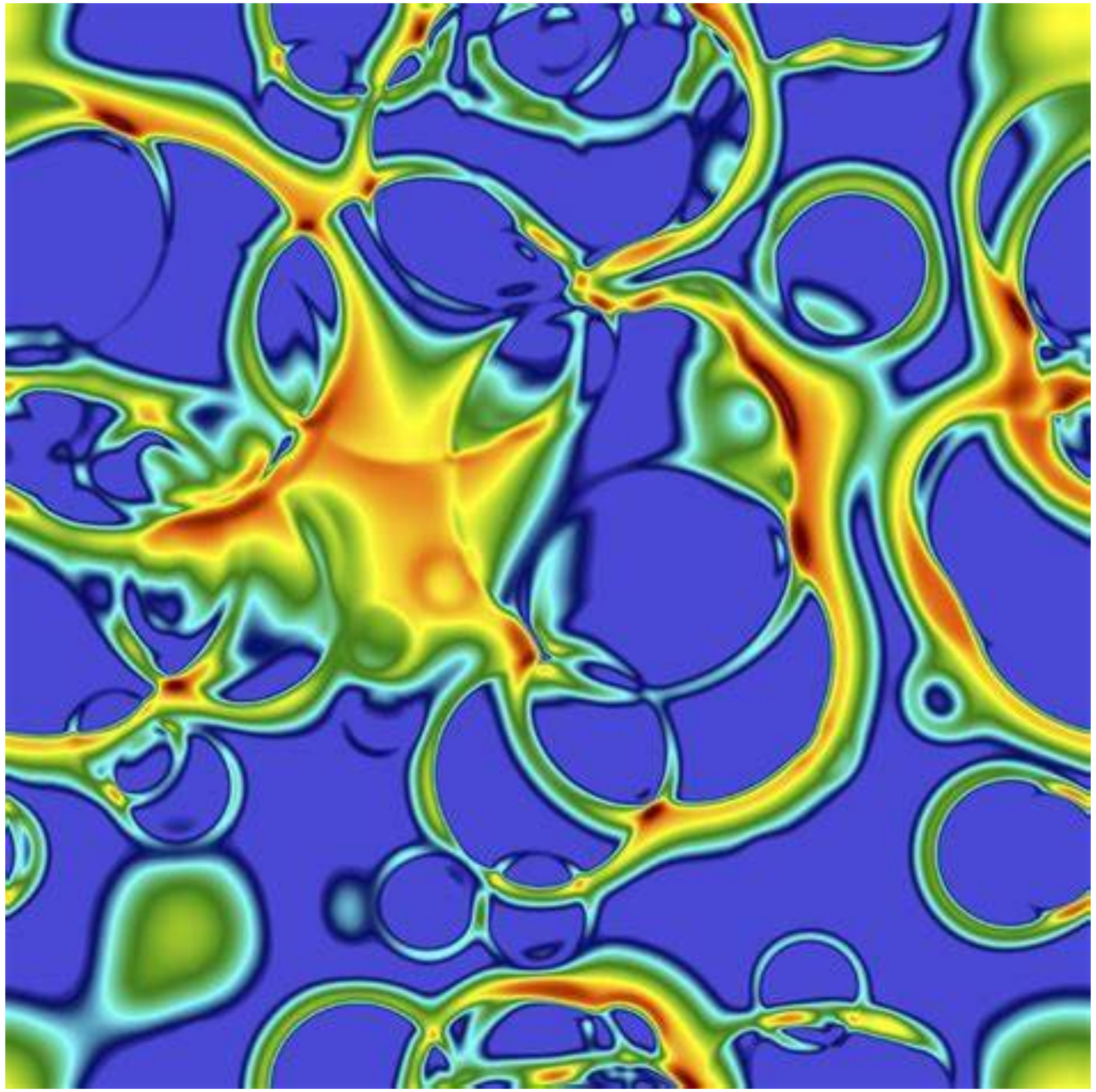

Credit to D. Weir, saoghal.net/slides/brda

How
necessarily new physics beyond the Standard Model.
Electroweak PT in minimal SM is a cross-over

Scalar field: Higgs or new particle

Higher order effective operators, example a D=6 self-interaction of the scalar field
It may be generated integrating out heavier fields or non-perturbative effects in composite Higgs models

Multi-scalar models. For example, Higgs strongly coupled with a scalar field.
In this case, a multi-step PT is possible

M. Hindmarsh, S. J. Huber, K. Rummukainen, and D. J. Weir, C. Caprini and R. Durrer and others

When

Cosmological time related to thermal history

Enucleation temperature
related to vacuum expectation value of the scalar field
and typically not far from it (there are exceptions such as in supercooled FOPTs)

Tunneling from false to true vacuum
Bubble enucleations

Gravitational waves stochastic background
Frequency peaks proportional to the temperature.
Higher is temperature higher the Frequency peak
3 contributions: collisions, sound waves and turbulence

M. Hindmarsh, S. J. Huber, K. Rummukainen, and D. J. Weir, C. Caprini and R. Durrer and others

$$\hat{S}_3(\hat{\phi}, T) = 4\pi \int_0^\infty \mathrm{d}r\, r^2 \left\{ \frac{1}{2} \left(\frac{\mathrm{d}\hat{\phi}}{\mathrm{d}r} \right)^2 + V_{\mathrm{eff}}(\hat{\phi}, T) \right\} ,$$

$$\int_{T_n}^{T_c} \frac{dT}{T} \frac{\Gamma(T)}{H(T)^4} = 1 ,$$

$$\Gamma(T) \approx T^4 \left(\frac{\hat{S}_3}{2\pi T} \right)^{3/2} e^{-\hat{S}_3/T} .$$

$$\alpha = \frac{1}{\rho_\gamma} \left[\Delta V - \frac{T}{4} \left(\frac{\partial \Delta V}{\partial T} \right) \right] ,$$

Latent heat

$$\Delta V = V_i - V_f \text{ with } V_i \equiv V_{\mathrm{eff}}(\phi^i_{h,\sigma}; T_*) \text{ and } V_f \equiv V_{\mathrm{eff}}(\phi^f_{h,\sigma}; T_*)$$

$$\frac{\beta}{H} = T_* \frac{\partial}{\partial T} \left(\frac{\hat{S}_3}{T} \right) \Bigg|_{T_*} .$$

Enucleation rate scale

M. Hindmarsh, S. J. Huber, K. Rummukainen, and D. J. Weir, C. Caprini and R. Durrer and others

Primordial Gravitational Waves from FOPTs

Strong FOPTs are violent processes occurring in the early Universe and are expected to leave a signature in the form of a stochastic background of primordial GWs.

In the first approximation, the primordial stochastic GW background is statistically isotropic, stationary and Gaussian. Furthermore, both the + and the × polarizations are assumed to have the same spectrum and are mutually uncorrelated. The GW power spectrum is given in terms of the energy-density of the gravitational radiation per logarithmic frequency as

$$h^2\Omega_{\rm GW}(f) \equiv \frac{h^2}{\rho_c}\frac{\partial \rho_{\rm GW}}{\partial \log}$$

vS>vJ supersonic detonation,
Sound Wave Dominance in GW

$$v_{\rm J} = \frac{1}{1+\alpha}\left(c_s + \sqrt{\alpha^2 + \tfrac{2}{3}\alpha}\right).$$

$$f_{\rm peak} = 26 \times 10^{-6}\left(\frac{1}{HR}\right)\left(\frac{T_*}{100}\right)\left(\frac{g_*}{100\ {\rm GeV}}\right)^{\frac{1}{6}} {\rm Hz}\,,$$

$$h^2\Omega_{\rm GW}^{\rm peak} = 1.159 \times 10^{-7}\left(\frac{100}{g_*}\right)\left(\frac{HR}{\sqrt{c_s}}\right)^2 K^{\frac{3}{2}} \quad \text{for} \quad {\rm H}\tau_{\rm sh} = \frac{2}{\sqrt{3}}\frac{\rm HR}{{\rm K}^{1/2}} < 1\,,$$

$$h^2\Omega_{\rm GW}^{\rm peak} = 1.159 \times 10^{-7}\left(\frac{100}{g_*}\right)\left(\frac{HR}{c_s}\right)^2 K^2 \quad \text{for} \quad {\rm H}\tau_{\rm sh} = \frac{2}{\sqrt{3}}\frac{\rm HR}{{\rm K}^{1/2}} \simeq 1\,,$$

$\tau_{\rm sh}$ is the fluid turnover time or the shock formation time.

R=mean bubble separation,
cs speed of sound

$$h^2\Omega_{\rm GW} = h^2\Omega_{\rm GW}^{\rm peak}\left(\frac{4}{7}\right)^{-\frac{7}{2}}\left(\frac{f}{f_{\rm peak}}\right)^3\left[1 + \frac{3}{4}\left(\frac{f}{f_{\rm peak}}\right)\right]^{-\frac{7}{2}},$$

$$K = \frac{\kappa\alpha}{1+\alpha} \qquad HR = \frac{H}{\beta}(8\pi)^{\frac{1}{3}}\max(v_b, c_s)\,.$$

Kinetic energy in the fluid from total bubble energy, depending from efficiency factor

M. Hindmarsh, S. J. Huber, K. Rummukainen, and D. J. Weir, C. Caprini and R. Durrer and others

Possible region of interest for FOPTs

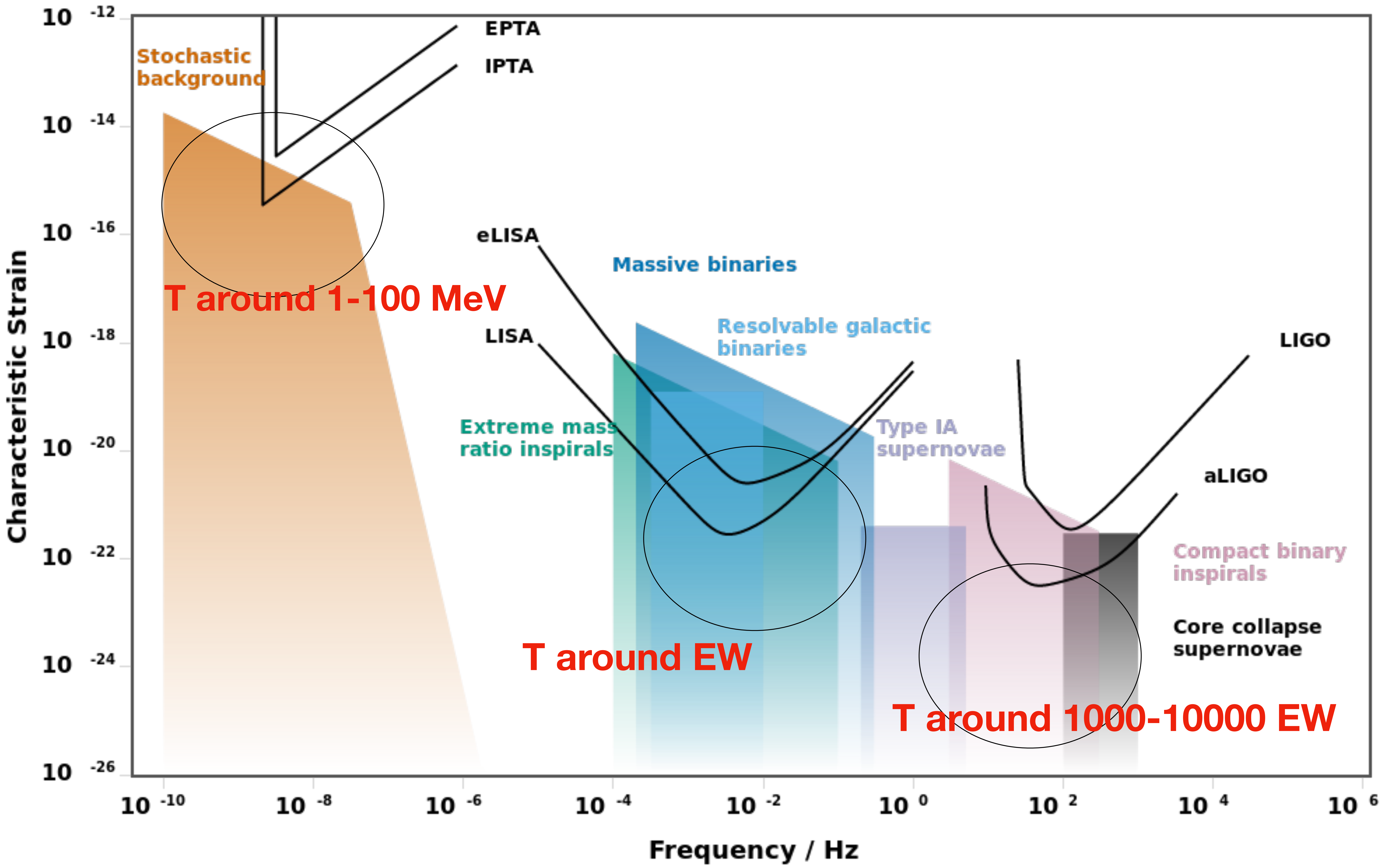

EW or around EW FOPTs

- D. E. Morrissey and M. J. Ramsey-Musolf, (2012), 1206.2942.
- D. Land and E. D. Carlson, Phys.Lett. **B292**, 107 (1992), hep-ph/9208227.
- A. Hammerschmitt, J. Kripfganz, and M. Schmidt, Z.Phys. **C64**, 105 (1994), hep-ph/9404272.
- S. Profumo, M. J. Ramsey-Musolf, and G. Shaughnessy, JHEP **0708**, 010 (2007), 0705.2425.
- H. H. Patel and M. J. Ramsey-Musolf, (2012), 1212.5652.

And many others …

…and efficient way to do that…

Higgs + complex scalar singlet

$$V_0(H,\sigma) = V_{\rm SM}(H) + V_{\rm 4D}(H,\sigma) + V_{\rm 6D}(H,\sigma) + V_{\rm soft}(\sigma)\,,$$

$$V_{\rm SM}(H) = \mu_h^2 H^\dagger H + \lambda_h (H^\dagger H)^2\,,$$
$$V_{\rm 4D}(H,\sigma) = \mu_\sigma^2 \sigma^\dagger\sigma + \lambda_\sigma(\sigma^\dagger\sigma)^2 + \lambda_{\sigma h} H^\dagger H \sigma^\dagger\sigma\,,$$
$$V_{\rm 6D}(H,\sigma) = \frac{\delta_0}{\Lambda^2}(H^\dagger H)^3 + \frac{\delta_2}{\Lambda^2}(H^\dagger H)^2\sigma^\dagger\sigma + \frac{\delta_4}{\Lambda^2}H^\dagger H(\sigma^\dagger\sigma)^2 + \frac{\delta_6}{\Lambda^2}(\sigma^\dagger\sigma)^3\,,$$
$$V_{\rm soft}(\sigma) = \frac{1}{2}\mu_b^2\left(\sigma^2 + \sigma^{*2}\right)\,.$$

$$H = \frac{1}{\sqrt{2}}\begin{pmatrix}\omega_1 + i\omega_2\\ \phi_h + h + i\eta\end{pmatrix}\,, \qquad \sigma = \frac{1}{\sqrt{2}}\left(\phi_\sigma + h' + iJ\right)\,,$$

The Majoron is the best candidate for it among pseudo-goldstone DM models QCD Axion for examples cannot have low scale spontaneous symmetry breaking of U(1)

Motivated as Warm Dark Matter if KeV mass

Typically the vev of U(1) can be around of lower than the electroweak scale
And actually this is theoretically preferable

Peccei, Mohapatra, Berezhinsky, Valle, Shekter, Akhmedov, Berezhiani, Dolgov, Senjanovic, Cline and many others

Motivated as Cold Dark Matter as Bose-Einstein condensate.
It may also mix with the QCD axion in a strong CP solution scenario

Valle et al;
For example if the Majoron is composite as in Dvali, Funcke et al

Majoron dark matter and neutrino mass in Standard see-saw, inverse see-saw and extended inverse see-saw type-I

	L^i	$\nu_{\rm R}^i$	S^i	σ	H	Model
	1	1	$\times$	-2	0	T1S
$\rm U(1)_L$	1	1	0	-1	0	IS
	1	1	-1	2	0	EIS

$$\mathcal{L}_\nu^{\rm T1S} = y_\nu^{ij}\overline{L}_i\tilde{H}\nu_{{\rm R}j} + y_\sigma^{ij}\bar{\nu}_{{\rm R}i}^c\nu_{{\rm R}j}\sigma + {\rm h.c.}\,,$$

$$\mathcal{L}_\nu^{\rm IS} = y_\nu^{ij}\overline{L}_i\tilde{H}\nu_{{\rm R}j} + y_\sigma^{ij}\bar{S}_i^c\nu_{{\rm R}j}\sigma + \Lambda^{ij}\bar{S}_i^c S_j + {\rm h.c.}\,,$$

$$\mathcal{L}_\nu^{\rm EIS} = y_\nu^{ij}\overline{L}_i\tilde{H}\nu_{{\rm R}j} + y_\sigma^{ij}\bar{S}_i^c S_j\sigma + y_\sigma'^{ij}\bar{\nu}_{{\rm R}i}^c\nu_{{\rm R}j}\sigma^* + \Lambda^{ij}\bar{\nu}_{{\rm R}i}^c S_j + {\rm h.c.}\,,$$

A. Addazi, R. Pasechnick, A. Marciano, A. Morais, R.Sivastrava, J.Valle, *Phys.Lett.B* 807 (2020) 135577;
AA, R. Pasechnick, A. Marciano, A. Morais, *JCAP* 09 (2023) 026.

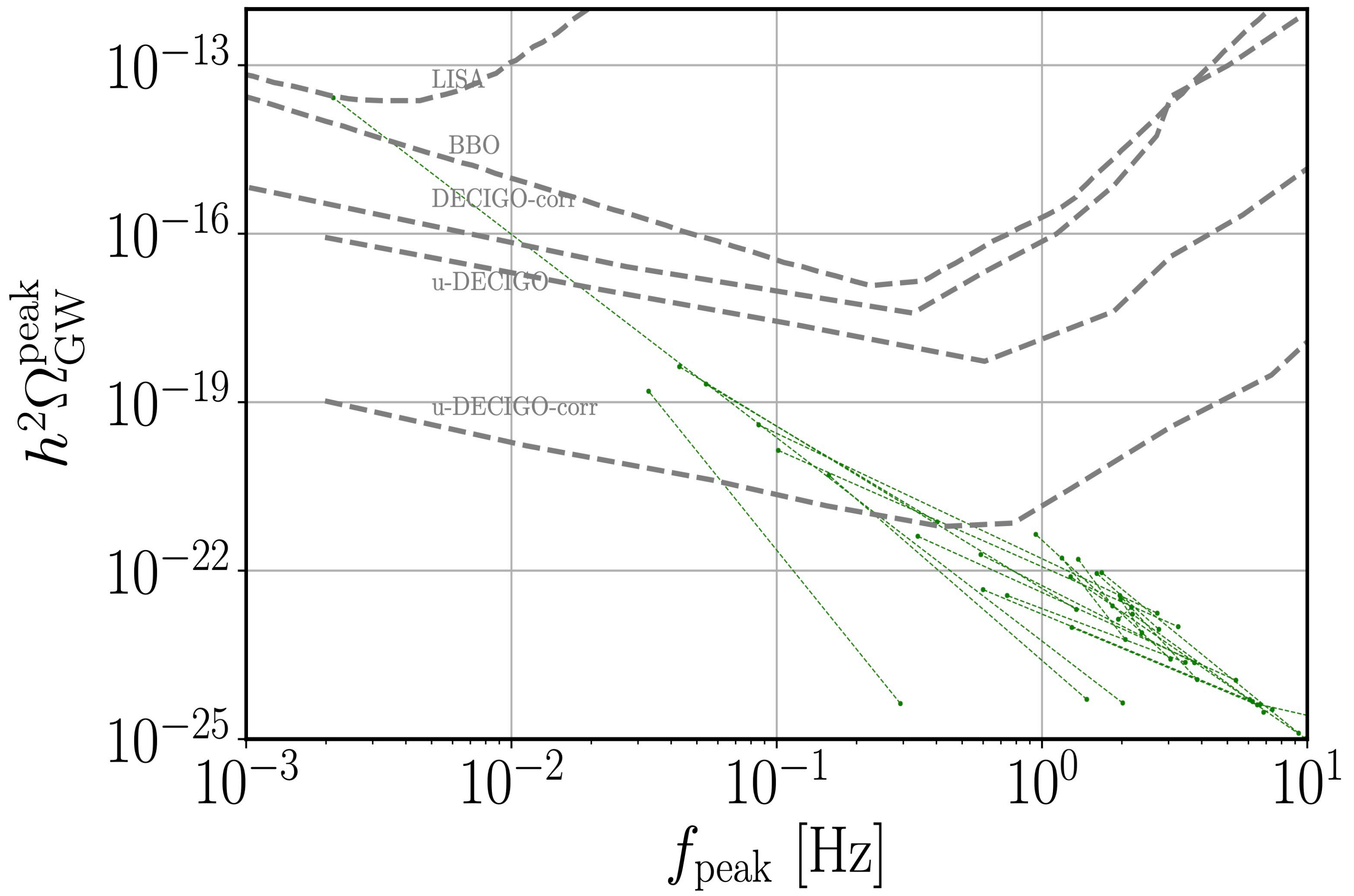

(a) Selected double-peak scenarios within the LISA and BBO sensitivity ranges. The two ends of each line represent the location of the peaks of the double-peak GW spectrum. The two maxima in each double-peak GW spectra are joined by a straight line, in order to easily identify the peaks associated with each other.

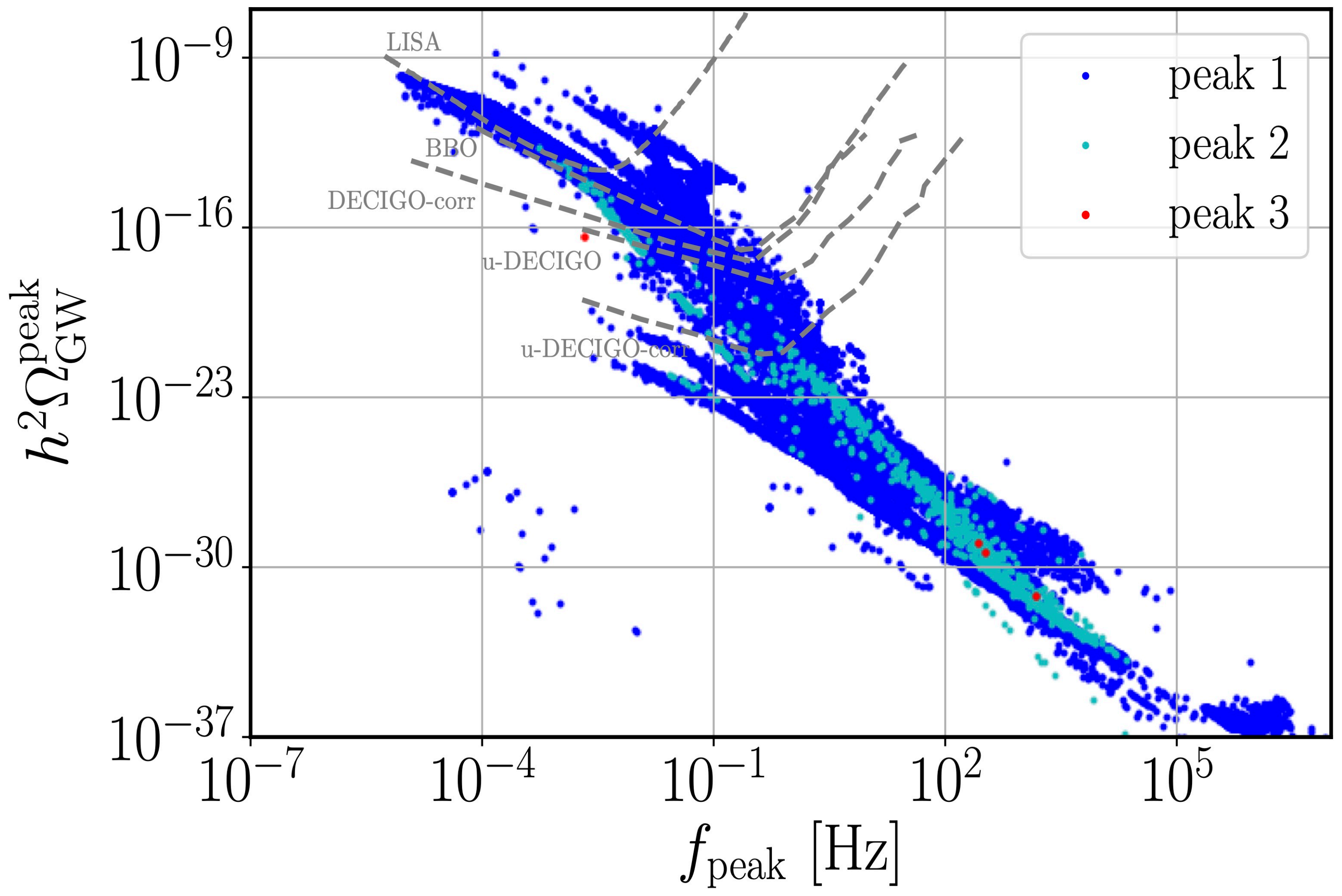

(b) Scatter plot showing the number of peaks for given model parameter choices. Notice the appearance of double- and even triple-peak features.

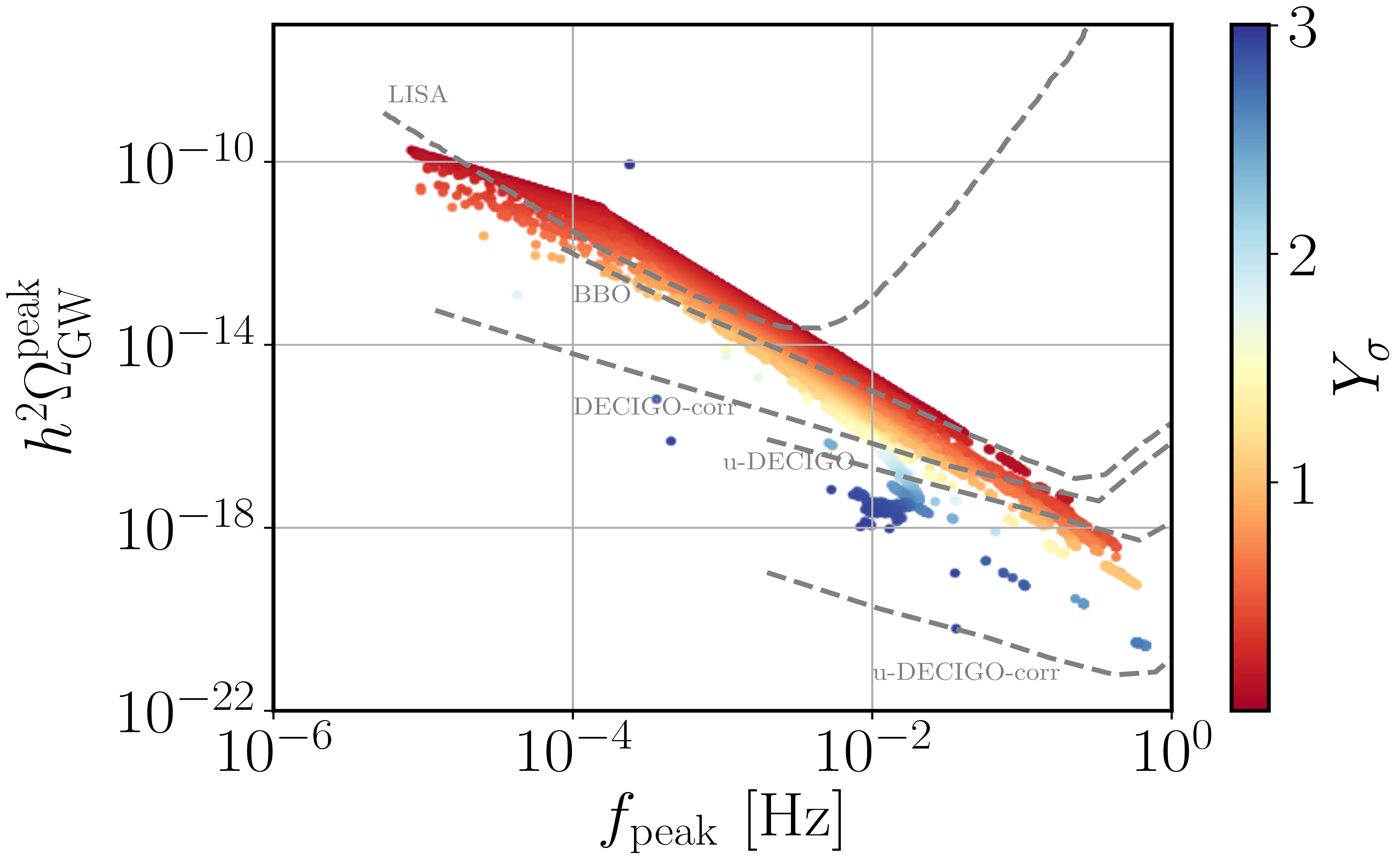

FIG. 2: The GW spectrum as a function of the Yukawa Y_σ coupling in the case of softly-broken $U(1)_L$ symmetry (i.e. $v_\sigma = 0$). Order one variation of Y_σ correspond to several order of magnitude variations in the GW power spectrum. Other model parameters are fixed as $\lambda_\sigma = 0.37$, $\lambda_{\sigma h} = 1.07$, $M = 239.4$ GeV, $m_{h_2} = 154.6$ GeV and $m_A = 369.9$ GeV.

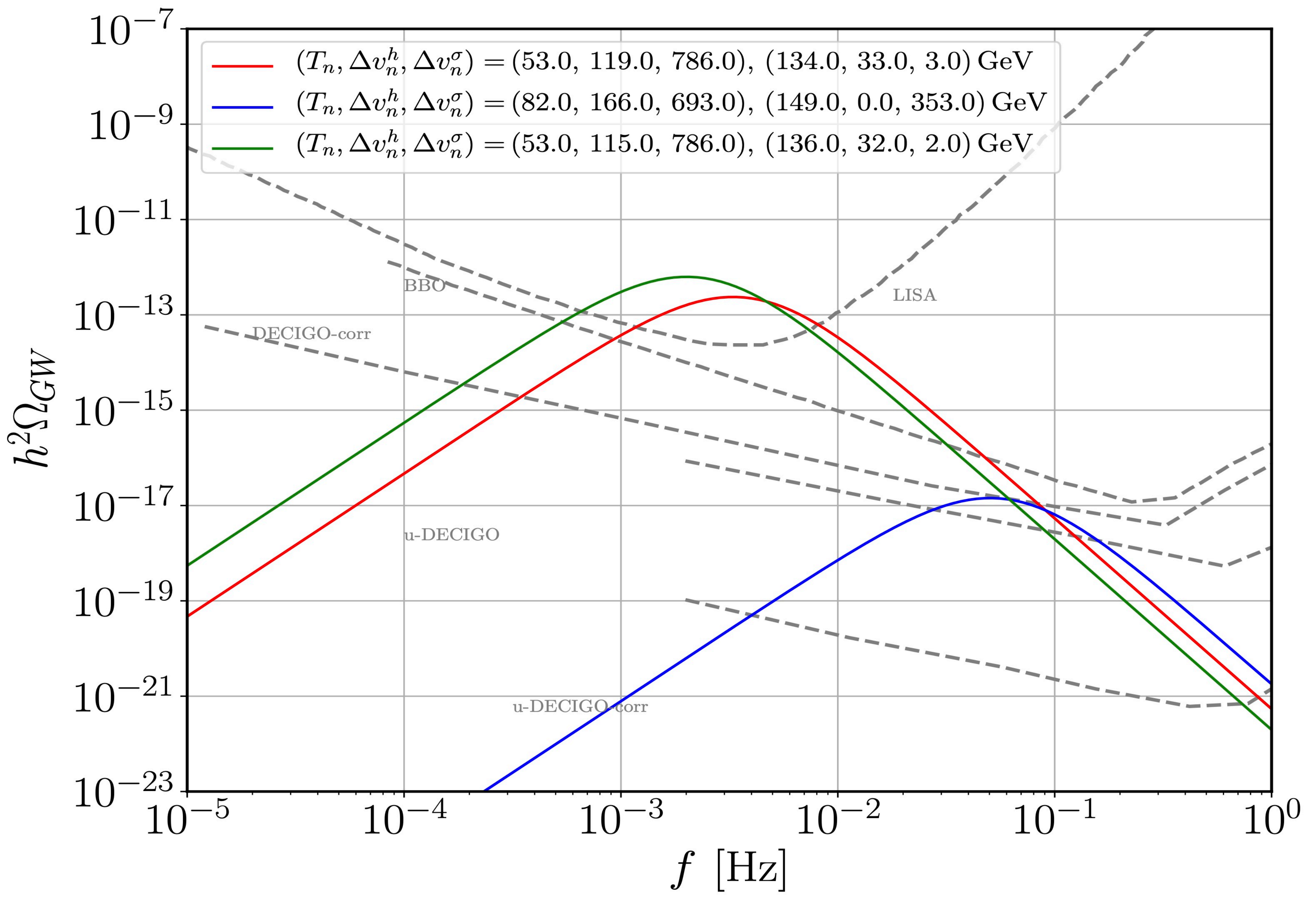

(a) The expected GW spectra.

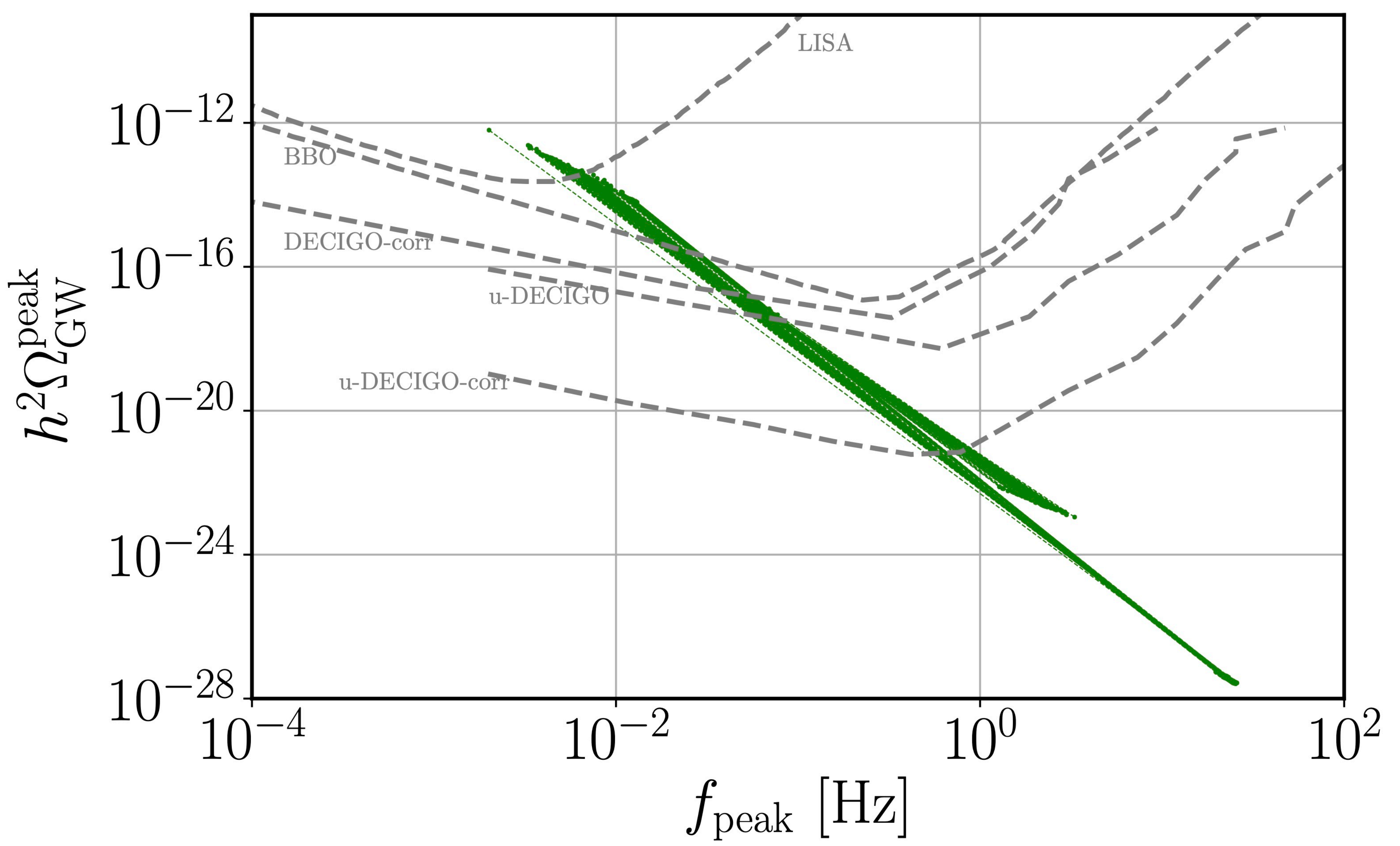

(b) Scatter plot showing typical double-peak scenarios.

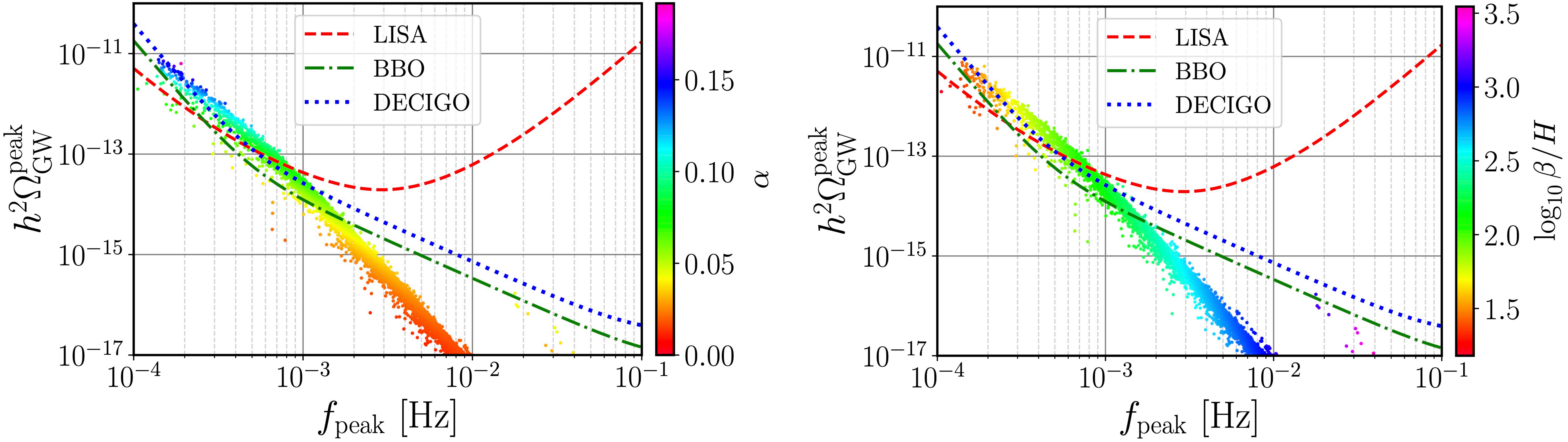
LISA
BBO
DECIGO
$h^2\Omega_{\rm GW}^{\rm peak}$
$f_{\rm peak}$ [Hz]
α
$\log_{10}\beta/H$

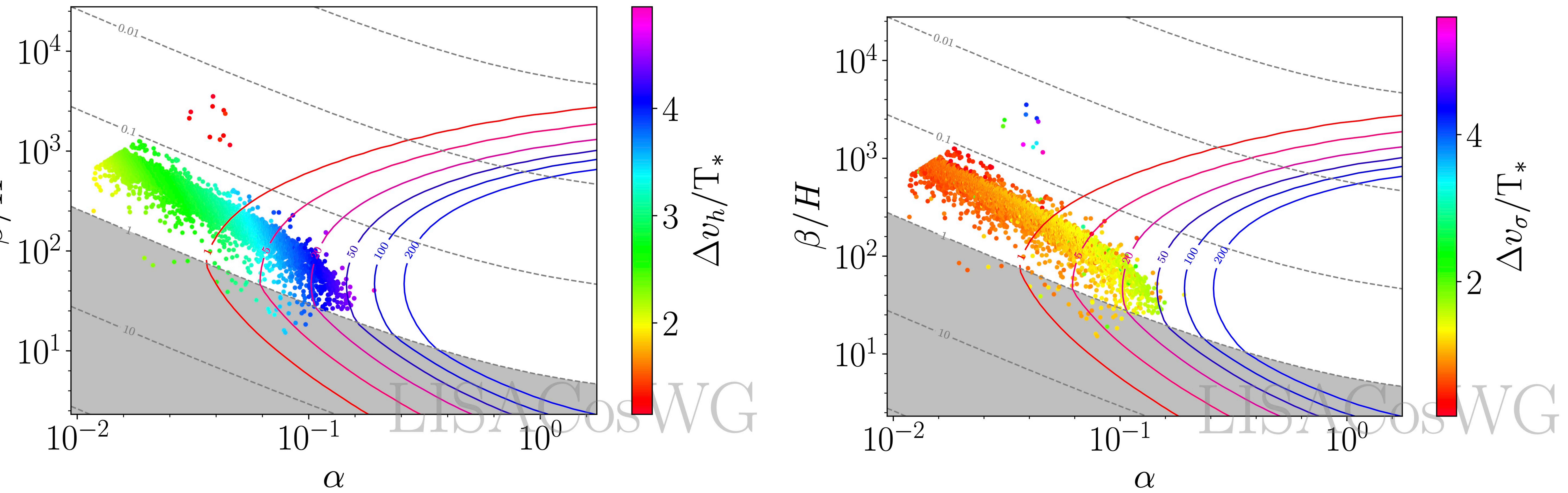

0.01
0.1
1
10
1
5
20
50
100
200
α
$\Delta v_h/T_*$
β/H
$\Delta v_\sigma/T_*$
LISACosWG

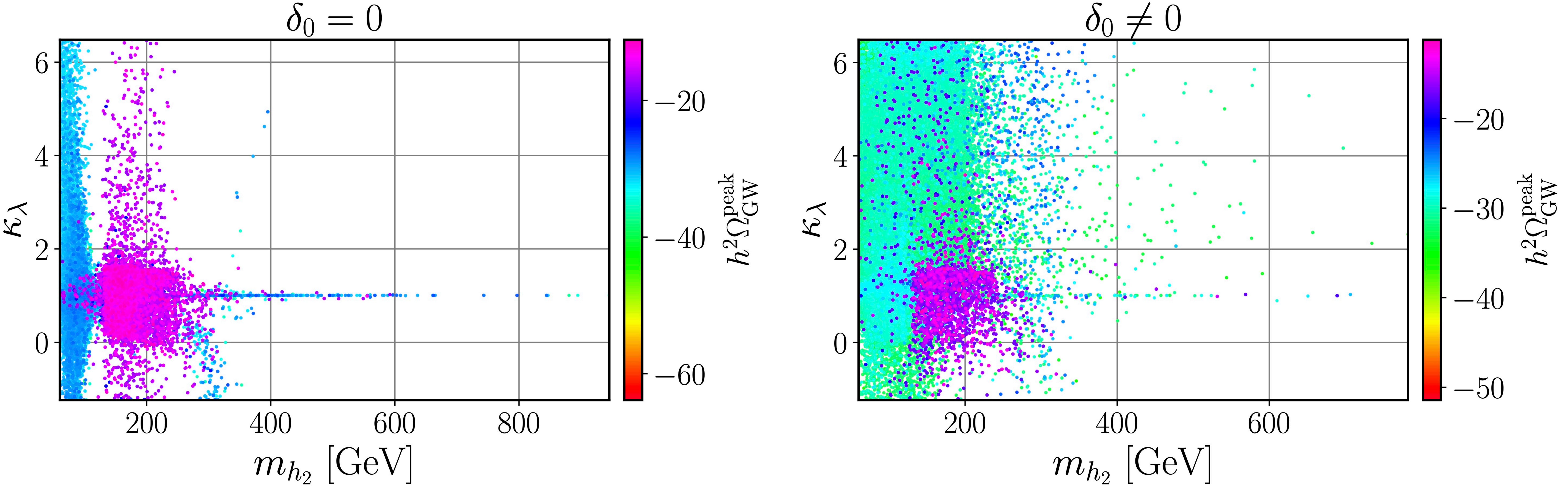

FIG. 4. Scatter plots showing the dependency of the Higgs trilinear coupling modifier in terms of the second CP-even Higgs boson mass and the energy density amplitude of the SGWB in the colour scale. In the left panel $\delta_0 = 0$ whereas in the right panel $\delta_0 \neq 0$.

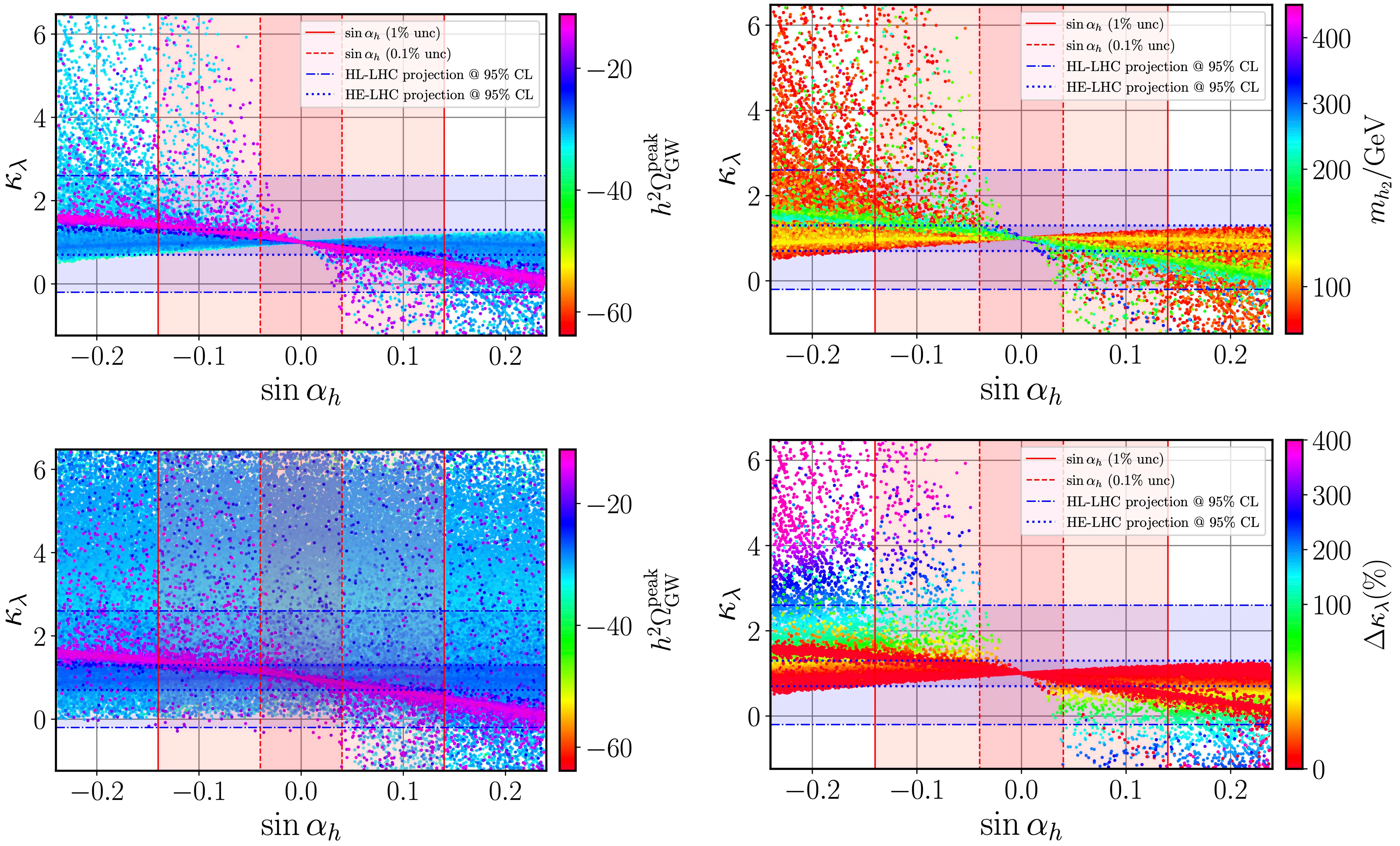

FIG. 6. Scatter plots showing the correlations between the Higgs trilinear coupling modifier κ_λ and the scalar mixing angle $\sin\alpha_h$. On both left panels, where the top one includes only $\delta_0 = 0$ data while the bottom one features all generated viable points, the colour scale denotes the energy density peak amplitude of the SGWB. On the top-right panel the colour gradient describes the mass of the new CP-even Higgs boson, h_2, and on the bottom-right one it quantifies the size of the one-loop contribution to the Higgs trilinear self coupling as defined in Eq. (5.4). The vertical red lines represent future constraints on $\sin\alpha_h$ assuming a precision of 1% (solid lines) and 0.1% (dashed lines) at future colliders [80]. The blue horizontal lines indicate the projected 95% CL limits in κ_λ measurements for the high-luminosity LHC (dot-dashed lines) and the future $\sqrt{s} = 27$ TeV high-energy upgrade (dotted lines) [82]. The regions under the darker blue and red shades correspond to the least constrained ones upon future measurements.

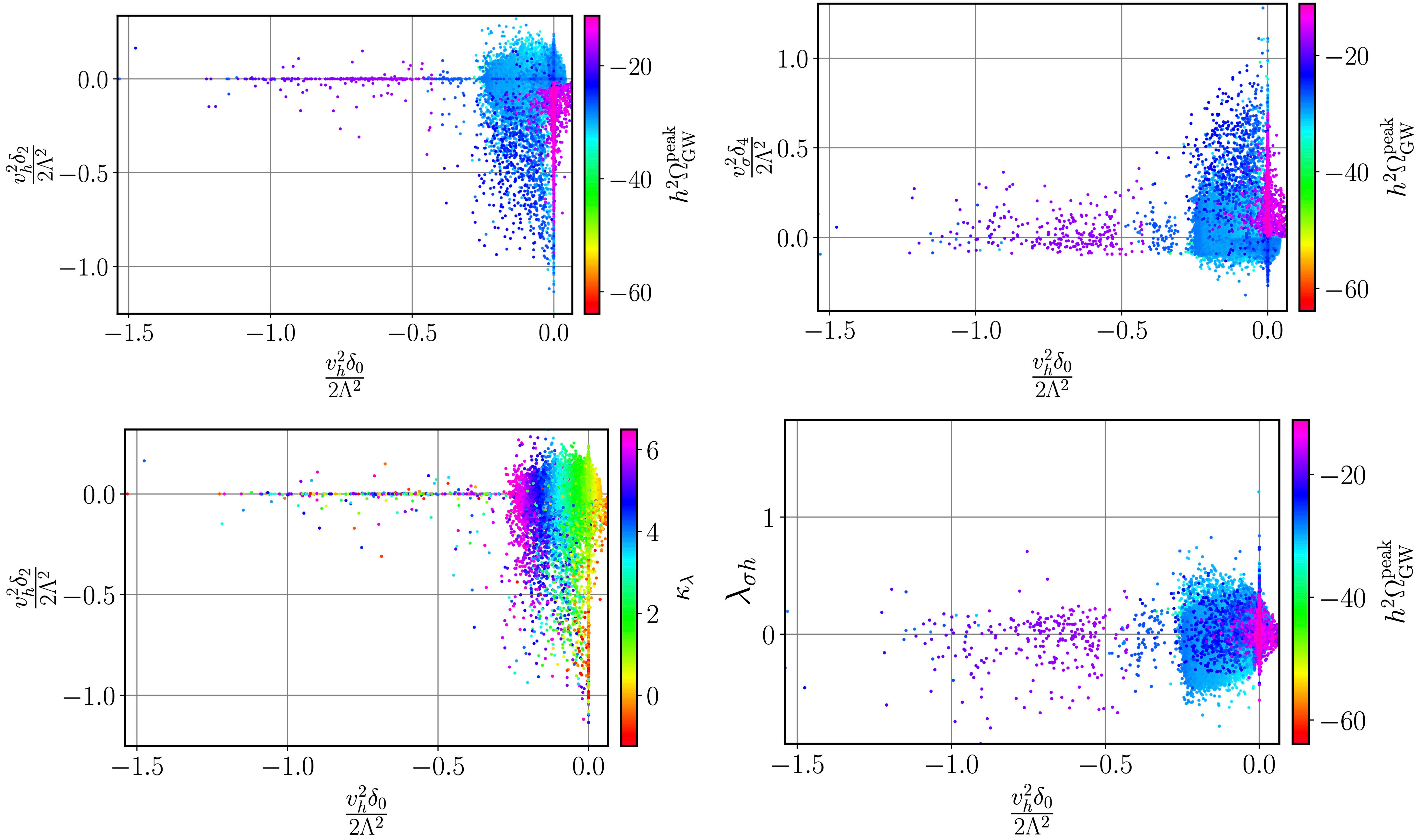

FIG. 5. Scatter plots showing the correlation between the strength of the Higgs self interaction $\frac{v_h^2\delta_0}{2\Lambda^2}$ and the effective portal couplings $\frac{v_h^2\delta_2}{2\Lambda^2}$ (both left panels), $\frac{v_\sigma^2\delta_4}{2\Lambda^2}$ (top-right) and $\lambda_{\sigma h}$ (bottom-right). The SGWB peak amplitude is shown in the colour scale of the top and bottom-right panels, while in the bottom-right we show the trilinear Higgs coupling modifier.

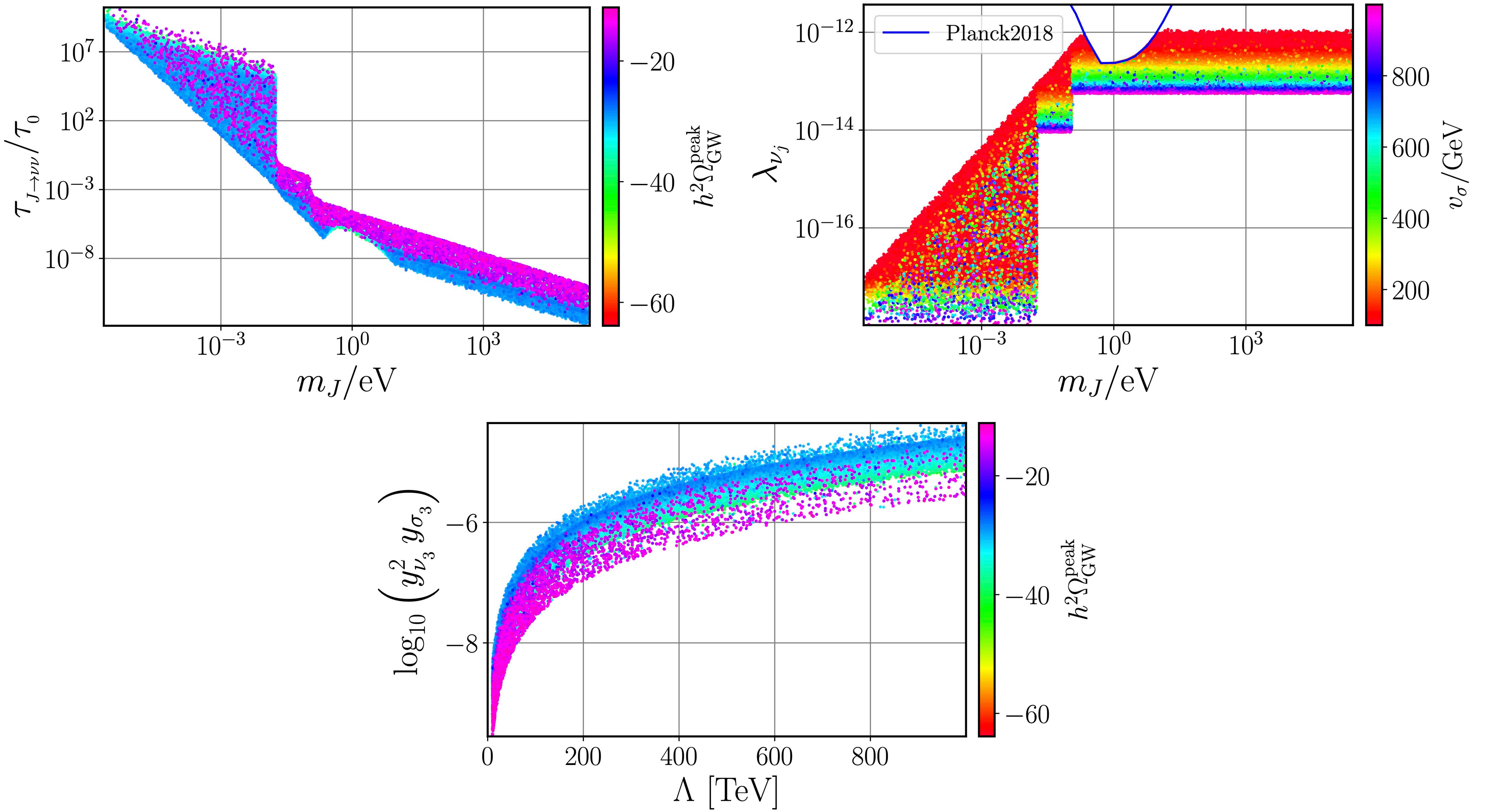

FIG. 7. Scatter plots showing the Majoron decay life-time normalized to the age of the Universe τ_0 in terms of the Majoron mass and the SGWB peak amplitude (top-left), the strength of the neutrino coupling to Majorons versus the Majoron mass and the $\mathrm{U}(1)_{\mathrm{L}}$ lepton number symmetry breaking scale (top-right), and the third generation nutrino Yukawa couplings in terms of the heavy neutrinos mass scale and the amplitude of the SGWB (bottom).

A1: one-loop T-dependent effective potential

$$V_{\rm eff}(T) = V_0 + V_{\rm CW}^{(1)} + \Delta V(T) + V_{\rm ct}\,,$$

Effective Potential

Ref, Quiros 1999, hep-ph/9901312.

$$V_{\rm CW}^{(1)} = \sum_i (-1)^{F_i} n_i \frac{m_i^4(\phi_\alpha)}{64\pi^2}\left(\log\left[\frac{m_i^2(\phi_\alpha)}{Q^2}\right] - c_i\right)\,,$$

Coleman-Weinberg 1-loop potential (Landau Gauge)

Field dependent masses, n are d.o.f for each i-species, Q is the renormalisation sale, ci=3/2(all except:),1/2(transv.gaugebosons) in MSbar scheme

$$V_{\rm ct} = \frac{\partial V_0}{\partial p_i}\delta_{p_i}\,,$$

Counter-term potential

$$\left\langle \frac{\partial V_{\rm ct}}{\partial \phi_i}\right\rangle = \left\langle -\frac{\partial V_{\rm CW}^{(1)}}{\partial \phi_i}\right\rangle\,, \qquad \left\langle \frac{\partial^2 V_{\rm ct}}{\partial \phi_i \partial \phi_j}\right\rangle = \left\langle -\frac{\partial^2 V_{\rm CW}^{(1)}}{\partial \phi_i \partial \phi_j}\right\rangle\,, \qquad \text{with} \qquad \phi_i = \{\phi_h, \phi_\sigma\}\,,$$

The counter-terms are introduced to guarantee That masses at 1-loop are the same of tree-level

$$\begin{aligned}
\delta_{\mu_h^2} &= \frac{1}{2}\frac{\partial^2 V_{\rm CW}^{(1)}}{\partial v_h^2} + \frac{1}{2}\frac{v_\sigma}{v_h}\frac{\partial^2 V_{\rm CW}^{(1)}}{\partial v_h \partial v_\sigma} - \frac{3}{2}\frac{1}{v_h}\frac{\partial V_{\rm CW}^{(1)}}{\partial v_h} + a\frac{3}{4}\frac{v_h^4}{\Lambda^2} + b\frac{1}{2}\frac{v_h^2 v_\sigma^2}{\Lambda^2} + c\frac{1}{4}\frac{v_\sigma^4}{\Lambda^2}\,,\\
\delta_{\mu_\sigma^2} &= \frac{1}{2}\frac{\partial^2 V_{\rm CW}^{(1)}}{\partial v_\sigma^2} + \frac{1}{2}\frac{v_h}{v_\sigma}\frac{\partial^2 V_{\rm CW}^{(1)}}{\partial v_h \partial v_\sigma} - \frac{3}{2}\frac{1}{v_\sigma}\frac{\partial V_{\rm CW}^{(1)}}{\partial v_\sigma} + b\frac{1}{4}\frac{v_h^4}{\Lambda^2} + c\frac{1}{2}\frac{v_h^2 v_\sigma^2}{\Lambda^2} + d\frac{3}{4}\frac{v_\sigma^4}{\Lambda^2} - f\,,\\
\delta_{\lambda_h} &= -\frac{1}{2}\frac{1}{v_h^2}\frac{\partial^2 V_{\rm CW}^{(1)}}{\partial v_h^2} + \frac{1}{2}\frac{1}{v_h^3}\frac{\partial V_{\rm CW}^{(1)}}{\partial v_h} - a\frac{3}{2}\frac{v_h^2}{\Lambda^2} - b\frac{1}{2}\frac{v_\sigma^2}{\Lambda^2}\,,\\
\delta_{\lambda_\sigma} &= -\frac{1}{2}\frac{1}{v_\sigma^2}\frac{\partial^2 V_{\rm CW}^{(1)}}{\partial v_\sigma^2} + \frac{1}{2}\frac{1}{v_\sigma^3}\frac{\partial V_{\rm CW}^{(1)}}{\partial v_\sigma} - c\frac{1}{2}\frac{v_h^2}{\Lambda^2} - d\frac{3}{2}\frac{v_\sigma^2}{\Lambda^2}\,,\\
\delta_{\lambda_{\sigma h}} &= -\frac{1}{v_h v_\sigma}\frac{\partial^2 V_{\rm CW}^{(1)}}{\partial v_h \partial v_\sigma} - b\frac{v_h^2}{\Lambda^2} - c\frac{v_\sigma^2}{\Lambda^2}\,,\\
\delta_{\delta_0} &= a\,, \quad \delta_{\delta_2} = b\,, \quad \delta_{\delta_4} = c\,, \quad \delta_{\delta_6} = d\,, \quad \delta_{\mu_b^2} = f\,,
\end{aligned}$$

Resummation via Daisy or Ring diagram for Finite temperature potential

L. Dolan and R. Jackiw (1974);
R. Parwani (1992);P. B. Arnold and O. Espinosa (1993); J. R. Espinosa and M. Quiros, (1995);
D. Croon, O. Gould, P. Schicho, T. V. I. Tenkanen, and G. White (2021);
P. Schicho, T. V. I. Tenkanen, and G. White (2022);

$$\mu_\alpha^2(T) = \mu_\alpha^2 + c_\alpha T^2 \, . \qquad c_\alpha = \frac{\partial \Delta V^{(1)}(T,\phi_h,\phi_\sigma)^2}{\partial^2 \phi_\alpha} \, ,$$

where for the 6D EIS model one has

$$c_h = \frac{3}{16} g^2 + \frac{1}{16} g'^2 + \frac{1}{2}\lambda_h + \frac{1}{12}\lambda_{\sigma h} + \frac{1}{4}\sum_q y_q^2 + \frac{1}{12}\sum_\ell y_\ell^2 + \frac{1}{24} K_\nu + K_\Lambda^h \, ,$$

$$c_\sigma = \frac{1}{3}\lambda_\sigma + \frac{1}{6}\lambda_{\sigma h} + \frac{1}{24} K_\sigma + K_\Lambda^\sigma \, ,$$

$$K_\nu = \sum_{i=1}^{3} y_{\nu_i}^{\rm eff} \quad \text{with} \quad y_{\nu_i}^{\rm eff} = \frac{\phi_h \phi_\sigma}{2} \frac{y_{\nu_i}^2 y_{\sigma_i}}{\Lambda^2} \quad \text{and} \quad m_{\nu_i}(\phi_h) = \frac{\phi_h}{\sqrt{2}} y_{\nu_i}^{\rm eff} \qquad K_\sigma = \sum_{i=1}^{3} y_{\sigma_i}^2$$

$$K_\Lambda^h = \frac{3\phi_h^2}{\Lambda^2}\delta_0 + \frac{\phi_h^2 + \phi_\sigma^2}{4\Lambda^2}\delta_2 + \frac{\phi_\sigma^2}{6\Lambda^2}\delta_4 \qquad K_\Lambda^\sigma = \frac{\phi_h^2}{4\Lambda^2}\delta_2 + \frac{\phi_h^2}{6\Lambda^2}\delta_4 + \frac{\phi_\sigma^2}{2\Lambda^2}\delta_4 + \frac{9\phi_\sigma^2}{4\Lambda^2}\delta_6 \, .$$

Corrections to gauge boson masses $\{W_L^+, W_L^-, Z_L, A_L\}$

$$M^2_{\rm gauge}(\phi_h;T) = M^2_{\rm gauge}(\phi_h) + \frac{11}{6}T^2 \begin{pmatrix} g^2 & 0 & 0 & 0 \\ 0 & g^2 & 0 & 0 \\ 0 & 0 & g^2 & 0 \\ 0 & 0 & 0 & g'^2 \end{pmatrix},$$

whose eigenvalues of the zero-temperature mass matrix $M^2_{\rm gauge}(\phi_h)$ read as

$$m_W^2(\phi_h) = \frac{\phi_h^2}{4}g^2\,, \quad m_Z^2(\phi_h) = \frac{\phi_h^2}{4}(g^2+g'^2)\,.$$

Rotating to the physical basis one obtains the following mass spectrum

$$m^2_{W_L}(\phi_h;T) = m_W^2(\phi_h) + \frac{11}{6}g^2T^2\,,$$

$$m^2_{Z_L,A_L}(\phi_h;T) = \frac{1}{2}m_Z^2(\phi_h) + \frac{11}{12}(g^2+g'^2)T^2 \pm \mathcal{D}\,,$$

with the field-dependent W, Z boson masses given in Eq. (4.17), and

$$\mathcal{D}^2 = \left(\frac{1}{2}m_Z^2(\phi_h) + \frac{11}{12}(g^2+g'^2)T^2\right)^2 - \frac{11}{12}g^2g'^2T^2\left(\phi_h^2 + \frac{11}{3}T^2\right).$$

$$\Delta V(T) = \frac{T^4}{2\pi^2}\left\{\sum_b n_b J_B\left[\frac{m_b^2(\phi_\alpha)}{T^2}\right] - \sum_f n_f J_F\left[\frac{m_f^2(\phi_\alpha)}{T^2}\right]\right\},$$

$$J_{B/F}(y^2) = \int_0^\infty dx\, x^2 \log\left(1 \mp \exp[-\sqrt{x^2+y^2}]\right).$$

First non-trivial order of the Hessian matrix

$$\Delta V^{(1)}(T)|_{\text{L.O.}} = \frac{T^2}{24}\left\{\text{Tr}\left[M^2_{\alpha\beta}(\phi_\alpha)\right] + \sum_{i=W,Z,\gamma} n_i m_i^2(\phi_\alpha) + \sum_{i=\text{f}_i} \frac{n_i}{2} m_i^2(\phi_\alpha)\right\},$$

Where M is the scalar field dependent Hessian matrix

$$n_W = 6, \qquad n_Z = 3, \qquad n_\gamma = 2,$$

SM Gauge Bosons (W,Z and transversely polarised photon)

$$n_s = 6, \qquad n_{A_L} = 1,$$

Scalars and Longitudinally polarised photon

$$n_{u,d,c,s,t,b} = 12, \qquad n_{e,\mu,\tau} = 4, \qquad n_{\nu_{1,2,3}} = n_{N^\pm_{1,2,3}} = 2.$$

fermions

The Majoron model for FOPTs can be tested in colliders

Higgs trilinear couplings

Higgs decay into invisible channels

Interest for LHC in high luminosity phase or possible future electron positron colliders such as CEPC and so on.

A. Addazi, R. Pasechnick, A. Marciano, A. Morais, R.Sivastrava, J.Valle, *Phys.Lett.B* 807 (2020) 135577;
AA, R. Pasechnick, A. Marciano, A. Morais, *JCAP* 09 (2023) 026.

Implications to $0\nu\beta\beta - decay$

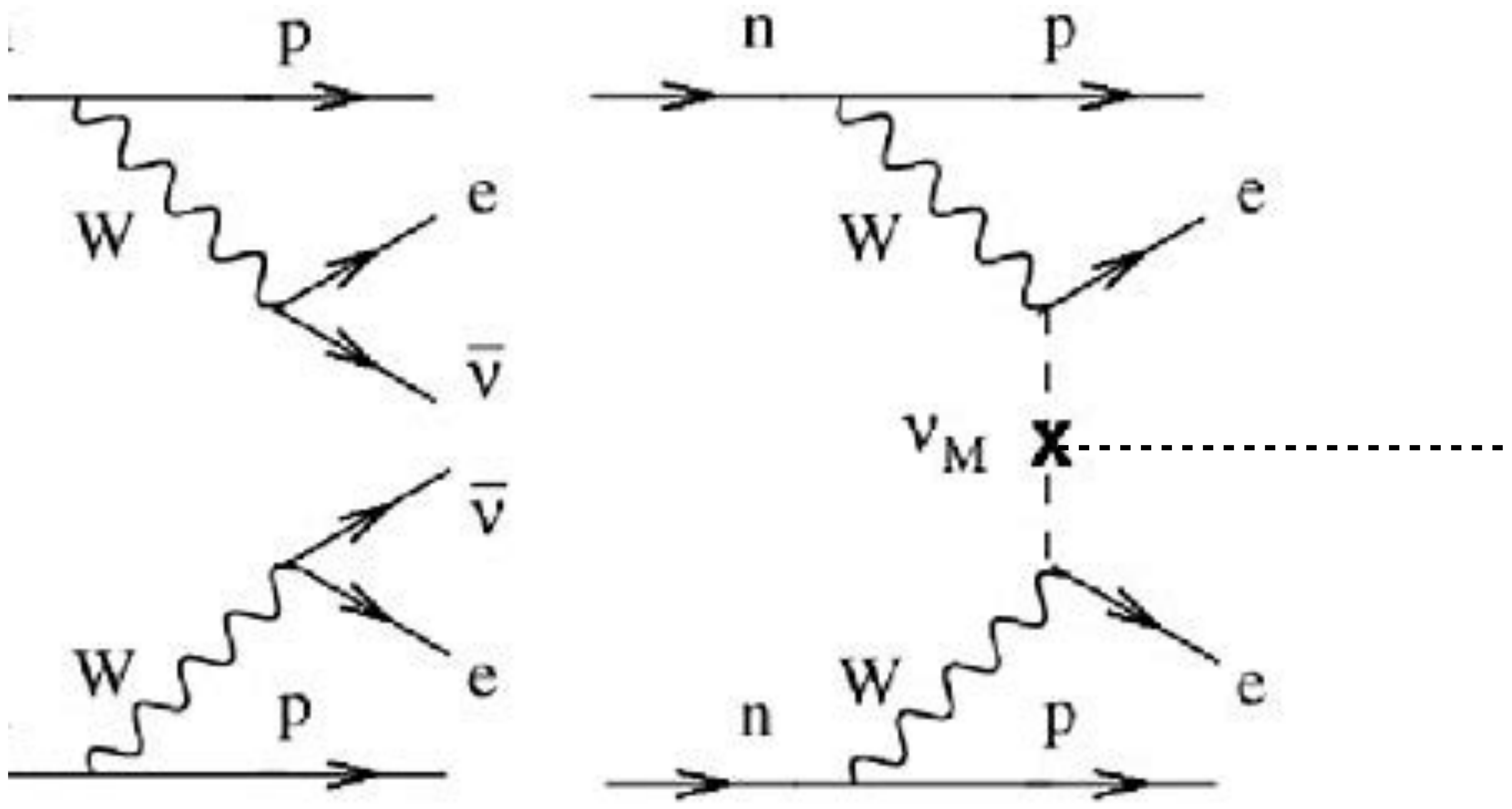

Majoron emissions,
See Jones arXiv:2108.09364v2
For an example of review

Possible prospectives: Local or global electroweak Baryogenesis in this scenario

In discussion with Michael Ramsey Musolf

Sub-electroweak FOPTs

Dark Matter Models

Majoron: extra global U(1)

AA. Y. Cai, A. Marciano et al

Dark Photon: extra gauge U(1)

AA, A. Marciano

Other possible dark symmetries …

Recent anomaly in NANOGrav-15yr, PPTA, EPTA, and CPTA

Compatible with sub-electroweak first order phase transitions
Alternative to Supermassive BH mergings

AA, Y. Cai, A.Marciano et al

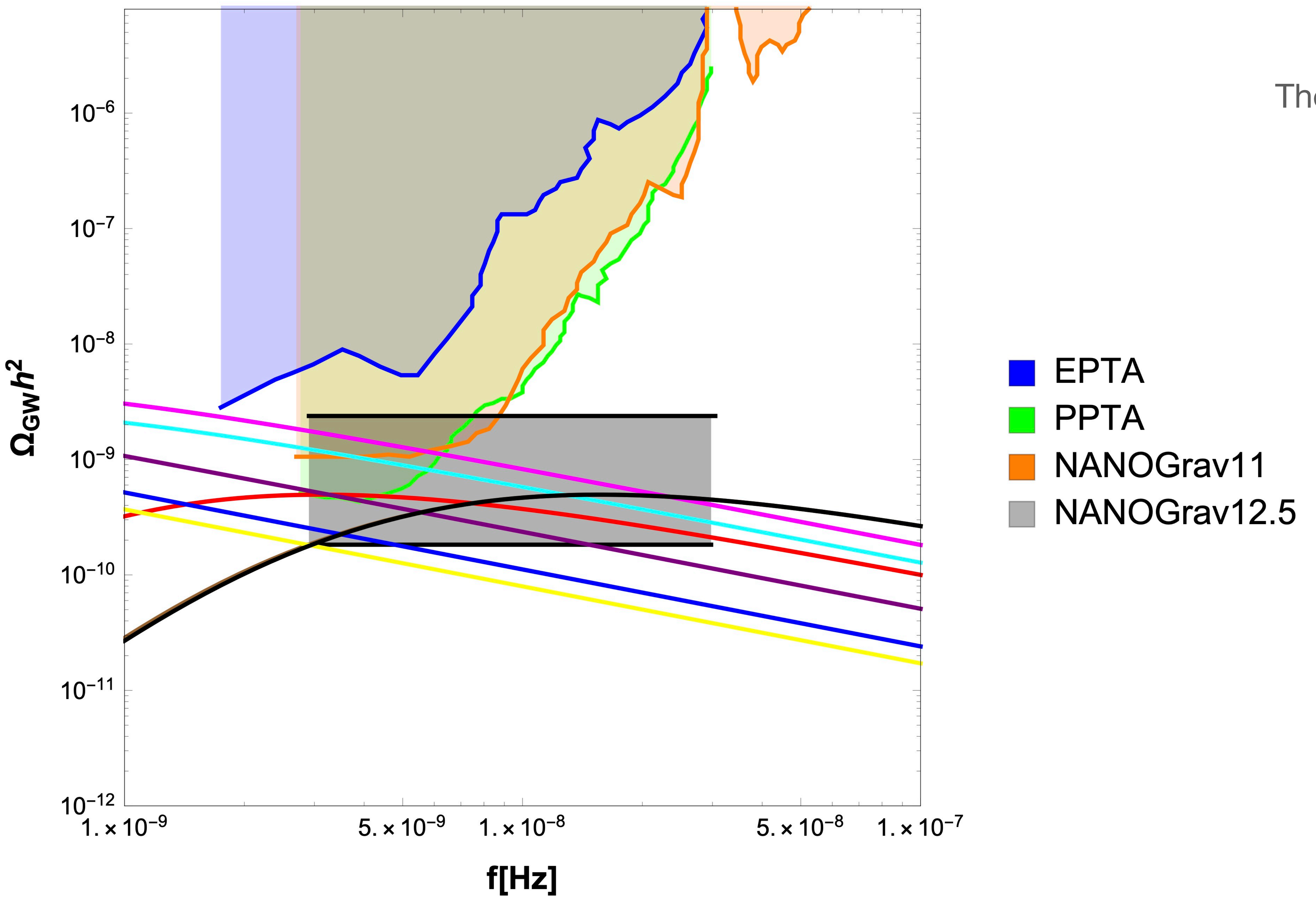

The 6D ope can work for It in Majoron model

$$\frac{1}{\Lambda^2}(\sigma^\dagger\sigma)^6$$

FIG. 1. Several GW signals from FOPTs are displayed and compared with the sensitivity region of NANOGrav 12.5 yrs [1], NANOGrav 11 yrs [52], PPTA [53], EPTA [54]. We show the cases of several FOPTs corresponding to different values of the $\{\alpha, \beta/H, T_n\}$ parameters: 1) Yellow $\{0.7, 5, 3\,\mathrm{KeV}\}$; 2) Cyan $\{0.3, 10, 300\,\mathrm{KeV}\}$; 3) Magenta $\{0.5, 2, 300\,\mathrm{KeV}\}$; 4) Blue $\{0.5, 2, 0.6\,\mathrm{KeV}\}$; 5) Dark purple $\{0.5, 10, 30\,\mathrm{KeV}\}$; 6) Red $\{0.1, 10, 2\,\mathrm{MeV}\}$, 7) Black $\{0.1, 10, 100\,\mathrm{MeV}\}$. The intrinsic uncertainties of sound and turbulence efficiency factors are considered.

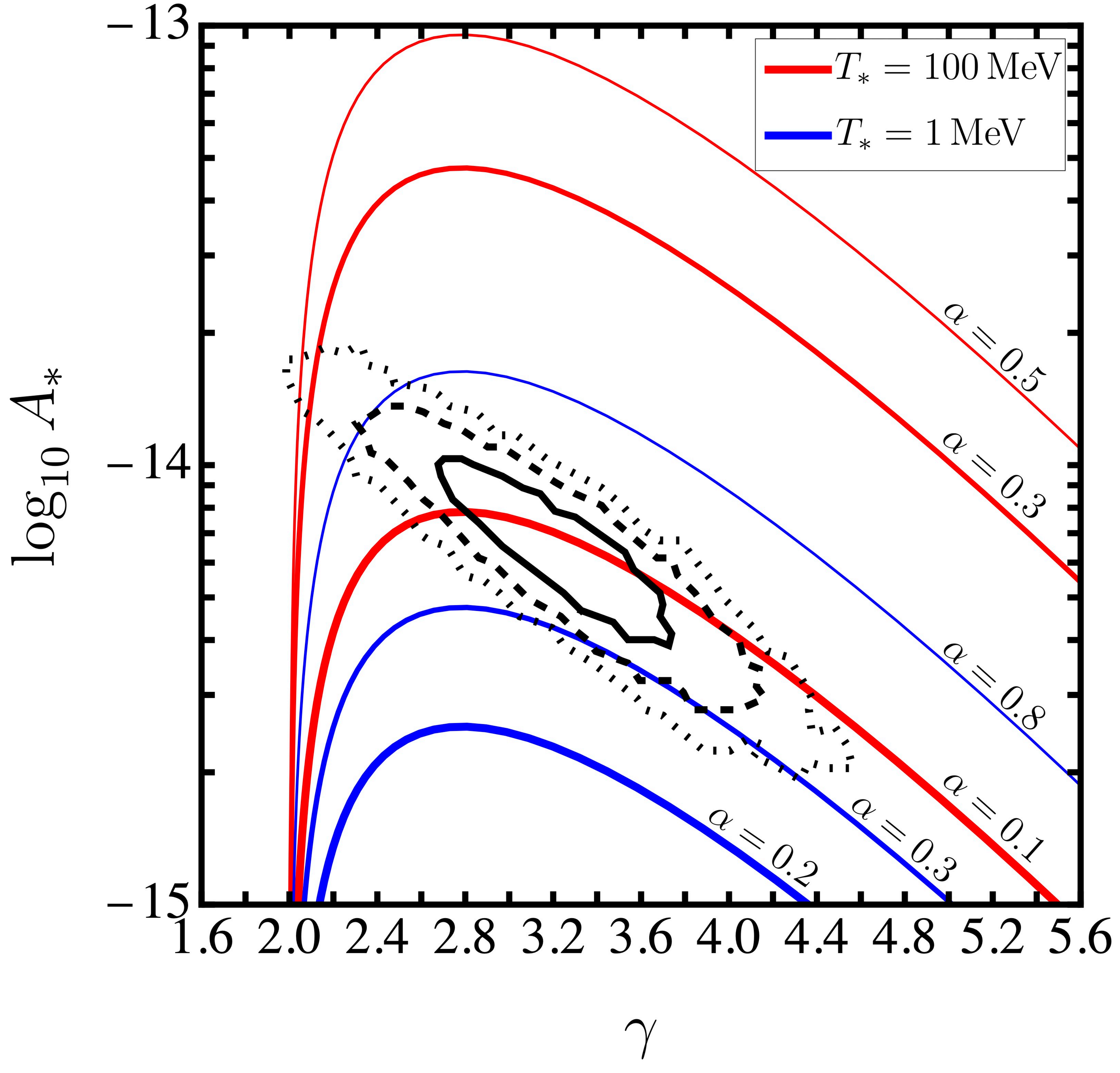

FIG. 1. The strain amplitude A_* (vertical axis) and the index γ (horizontal axis) predicted by different models of GWs from bubble collision for a phase transition occurring at $T_* = 100\,\mathrm{MeV}$ (red lines) and $T_* = 1\,\mathrm{MeV}$ (blue lines). Different line thicknesses correspond to different choices for the value of α — see the figure label for details. We also display the fit recently obtained by the NANOGrav collaboration [1] after analyzing the 15 years data set, with the different shadings marking the 1-, 2- and 3-σ confidence regions.

Neutron see-saw and new scalars: B-Majoron!

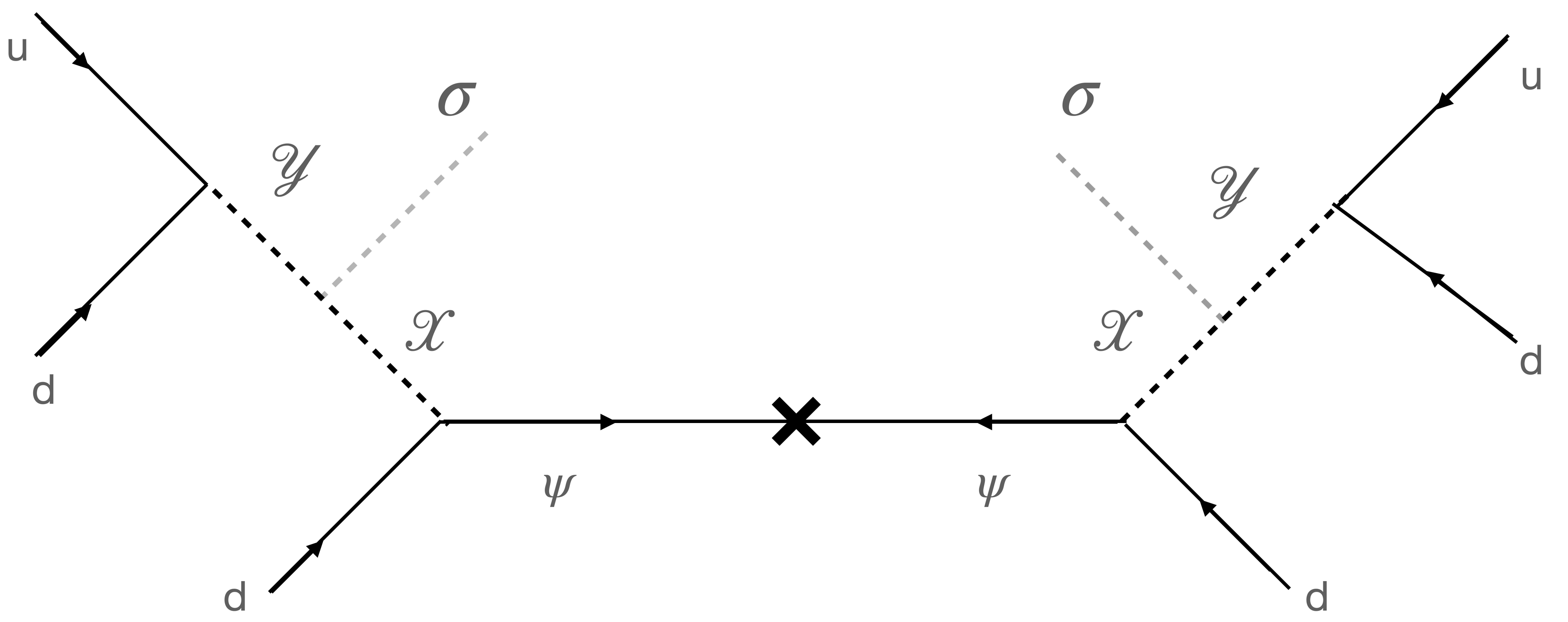

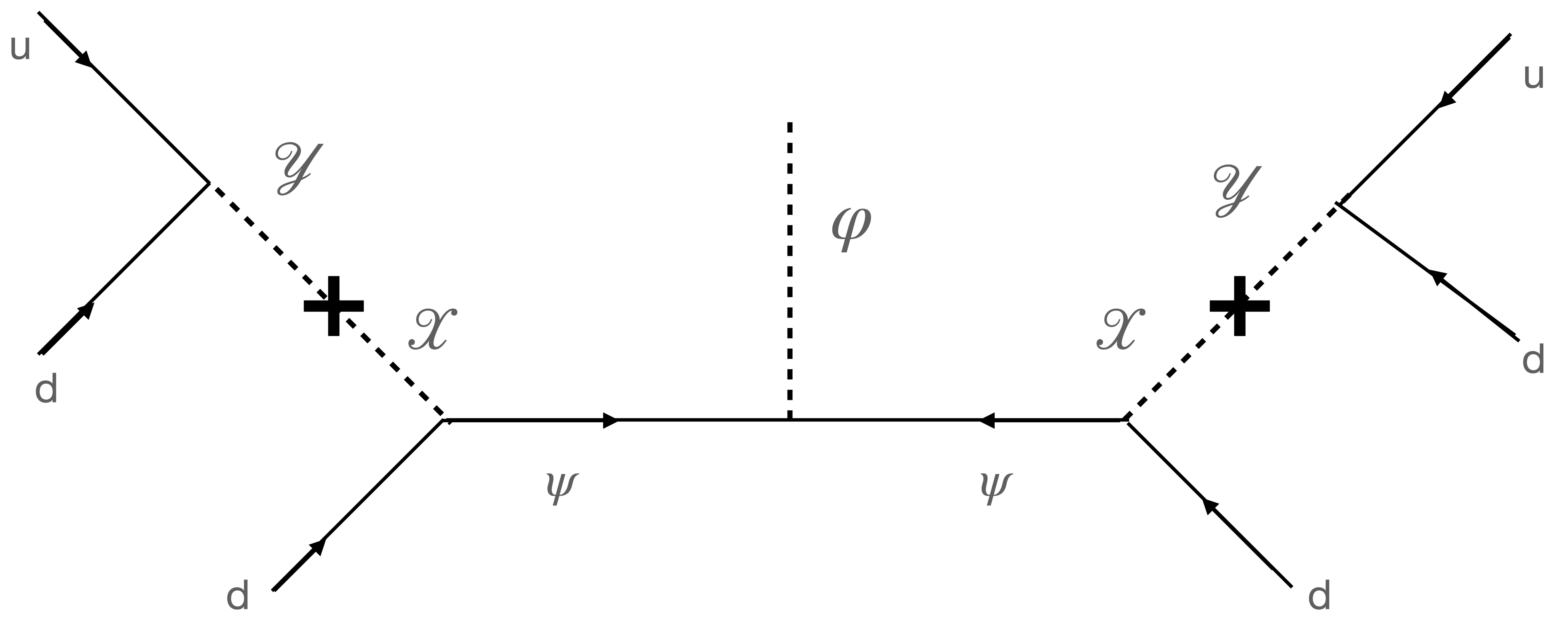

Z.Berezhiani,arXiv:1507.05478

A. Addazi arXiv:1501.04660 & work in progress

Thanks for the attention!